RSC Advances

ROYAL SOCIETY OF CHEMISTRY

www.rsc.org/advances

RSC Advances

RSCPublishing

ARTICLE

Magnetic behavior of the metal organic framework: $[(CH_3)_2NH_2]Co(HCOO)_3$

Cite this: DOI: 10.1039/xoxxoooooox

K. Vinod[a], C.S. Deepak[b], ShilpamSharma[a], D. Sornadurai[a], A.T Satya[a], T. R.Ravindran[a], C. S.Sundar[a] and A. Bharathi[a]

Received 22nd January 2015,
Accepted ooth January 2015

DOI: 10.1039/xoxxoooooox

www.rsc.org/

In this study we examine the phase transitions in single crystals of $[(CH_3)_2NH_2]Co(HCOO)_3$, using magnetization and specific heat measurements as a function of temperature and magnetic field. Magnetisation measurements indicate a transition at 15 K that is associated with an antiferromagnetic ordering. Isothermal magnetization versus magnetic field curves, demonstrate the presence of a single-ion magnet phase, coexisting with antiferromagnetism. A peak in specific heat is seen at 15 K, corresponding to the magnetic transition and the enthalpy of the transition evaluated from the area under the specific heat peak decreases with the application of magnetic field of upto 8 T. This is suggestive of long range antiferromagnetic magnetic order, giving way to single-ion magnetic behavior under external magnetic field. At high temperatures, the specific heat measurements, shows a peak at ~155 K, that is insensitive to applied magnetic field. Raman scattering studies confirm the presence of structural transition. The magnetisation in this temperature range, while it exhibits a paramagnetic behavior, shows a distinct jump and the paramagnetic susceptibility changes across the structural transition.

Introduction

The current interest in metal organic frameworks (MOF) stems from the enormous potential of their application in gas storage, catalysis, drug delivery, sensors, electronic devices, light emitting devices, and as an anode in Li-based batteries [1-5].The family of MOFs having a perovskite architecture, viz.,Di-Methylamine Metal Formamide, $[(CH_3)_2NH_2]M(HCOO)_3$ with M = Mn, Fe, Co and Ni, show couplings between their magnetic, dielectric and structural properties [6-10]. These compounds exhibit long range canted antiferromagnetic order at low temperatures[6]. Jain et al [7] have shown that in the Mn compound, there is a dielectric transition from paraelectric to an antiferroelectric phase, at ~ 160 K, coincident with a structural transition from a rhombohedral to monoclinic phase. The structure of $[(CH_3)_2NH_2]M(HCOO)_3$ is shown in the inset of Fig.1 the Co –O octahedra are linked via C-H of the formate. The organic $(CH_3)_2NH_2$ moiety is shown as a bi-pyramid, in the which the H atoms are not displayed. It is well known [7] that in– the high temperature disordered phase the nitrogen atom occupies one of the three positions, with equal probability. With decrease in temperature the nitrogen atom occupies a single position, leading to an ordering of nitrogen atom in the organic moiety $(CH_3)_2NH_2$ and to the structural change to a monoclinic phase. At low temperatures the magnetic moment on the Mn ion orders antiferromagnetically [7]. Specific heat measurements in the Mn compound [7] show anomalies at both 160 K and 8 K corresponding to the structural and magnetic transitions.

In a recent study on DMA– Fe – formamide single crystals, Tian et al [11] have shown the occurrence of a canted antiferromagnetic (AFM) transition at 20 K followed by a drop in magnetization at 8 K.They attribute this, to the behaviour of two co-existing magnetic phases corresponding to AFM order and a single ion magnet, showing resonant quantum tunnelling. The presence of two co-existing magnetic phases has been rationalized in terms of the structure (see Fig.1) that leads to two competing magnetic interactions of the Fe ions, one through the pure formate linker, and the other via the formate entity coupled with the DMA^+cation via a hydrogen bond (N-H…O). Dielectric constant measurements in this compound[12,13] shows an increase below the magnetic transition at 20 K, pointing to a magneto-electric coupling. The dielectric anomaly at the structural transition temperature of ~ 160 K is also affected by the application of external magnetic field. These results emphasise the cross coupling between electric and magnetic orders in $[(CH_3)_2NH_2]Fe(HCOO)_3$.

The aim of our study is to investigate phase transitions corresponding to magnetic order and order-disorder structural transition in the corresponding Co-formamide compound, viz., $[(CH_3)_2NH_2]Co(HCOO)_3$. These investigations were carried out to

see if the Co formamide compound bears any similarity to the Fe compound and also investigate if Co^{2+}, that has a propensity to exist in various spin states [14] has any influence on the observed phase transitions in the material. Towards this, we first synthesize single crystals of $[(CH_3)_2NH_2]Co(HCOO)_3$ by an already established route [7]. We investigate the magnetic property of the tiny single crystal using a SQUID vibrating sample magnetometer, in external magnetic fields of upto 6 Tesla. The magnetization measurements, are followed up with highly sensitive, specific-heat measurements, carried out on a 250 micron sized single crystal, by ac calorimetry, in the temperature range of 5 to 300 K, and in magnetic fields upto 8 T. These results point to the presence of two coexisting magnetic phases, as was seen in the Fe compound [11]. Further, the magnetization measurements across the order-disorder structural transition, shows a distinct jump, which could be attributed to a change in the magnetic moment of Co^{2+}.

Experimental

The synthesis of the Co compound was carried out using a solvothermal approach [7], in which 30 ml of di-methyl formamide and 30 ml of millipore water are taken in a 100 ml beaker into which 5 mmol of cobalt chloride, hexahydrate ($CoCl_2.6H_20$) was added. The crystals readily dissolve in this solution to give a deep pinkish red colour. This solution was filled into a Teflon lined autoclave and heated treated at 140 ^{0}C for 3 days. The furnace was switched off and the autoclave was allowed to remain in the furnace. The autoclave was removed from the furnace when it was at 42 ^{o}C and allowed to cool in air. After the autoclave was cooled to room temperature, it was opened and the supernatant was poured into another 100 ml beaker and left for three days, at ambient temperature. Crystals that form were primarily attached to the walls of the beaker. They were filtered and washed with alcohol. Shiny crystals of flat and cuboidal morphologies were seen to form, as discerned under the microscope. From powder XRD data, we could infer that the crystals with flat morphology were $Co(HCOO)_2.2H_20$ [15] and those with cuboidal morphology were $[(CH_3)_2NH_2]Co(HCOO)_3$. The crystals with cuboidal morphology (see inset Fig.1) were separated and used in further experiments. Powder XRD measurements at room temperature, was carried out in the BL-12 beam line of the Indus-2 synchrotron in Indore India, using 16 keV x-rays [16]. The powdered crystals were placed in a circular depression made on Kapton tape. The data was collected on a MAR3450 image plate detector in the transmission geometry. Fit2D program [17] was employed to convert the 2D image from the image plate detector to 1D Intensity versus 2θ plot. The experimental XRD pattern obtained is shown in the main panel of Fig.1. The diffraction data was consistent with trigonal structure of space group (R -3 c (167)). The lattice parameters, extracted employing the GSAS program [18, 19] are a =b = 8.2012$\pm$ 0.0007 A and c= 22.547$\pm$0.003 A. These values lie between those obtained for Fe and Zn formamide compounds [20], as is expected.The structure generated using the CASTEP programme is shown in the inset of Fig.1.

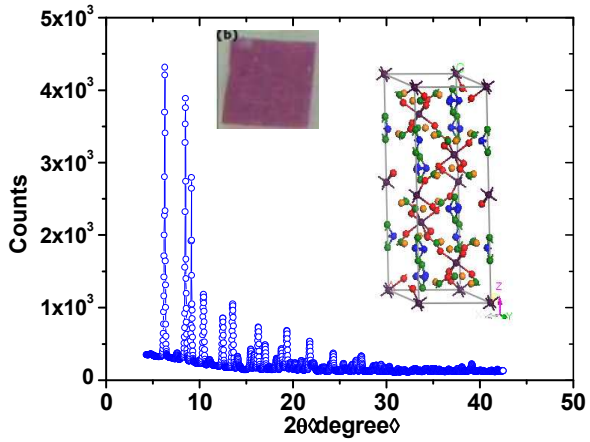

Fig.1XRD pattern of the powdered crystals $[(CH_3)_2NH_2]Co(HCOO)_3$ along with the schematic of the structure: Co (purple), O (orange), N (blue), C (green) and H (yellow). H atoms in the central organic moiety were removed for clarity. Top inset: optical microscope image of the crystal of lateral dimension ~0.2 mm used for the physical property measurements.

The magnetization measurements were carried out in a Quantum Design Ever-Cool SQUID vibrating sample magnetometer capable of a temperature variation of 1.6 K to 320 K and field variation of 0 to 7 Tesla, with a base sensitivity of 10^{-7} emu. These measurements were carried out in the zero field cooled (ZFC) and field cooled (FC) protocols. For the temperature scan during the ZFC and FC measurements, the temperature was varied at the rate of 2 K/min upto 50 K and at 8 K/min from 50 K up to 180 K. For the scans as a function of magnetic field the ramp rate of magnetic field was done at the rate of ~50 Oe/ s. The measurement of specific heat on the single crystal was carried out by ac calorimetry, in the 4 K to 300 K temperature range, in external fields upto to 8 Tesla, using a Cryogenic-make insert, to the existing vibrating sample magnetometer. In this ac calorimetric technique a sinusoidal current (11 Hz) is passed through a heater and the temperature rise is monitored by thermopiles phase sensitively [21]. The heater and the thermopiles are a part of a custom made chip and are in close proximity to the 250 micron sized crystal. The heat capacity using this system has a sensitivity of ~nJ/K, enabling measurement on very small crystals. The ramping of temperature for the heat capacity versus temperature measurements was done at a rate of 0.5 K/min.
Raman scattering investigations were done using Renishaw, UK, model inVia, micro- Raman set up, with an excitation wavelength of 488nm wavelength. The low temperature was achieved using a continuous flow cryostat using liquid nitrogen cryogen.

Results and discussions

For the magnetization measurements, a single cuboidal crystal of ~0.2x0.2x0.16 mm was placed on the puck of the sample holder in

which the face of the crystal (012), viz., the growth direction,was perpendicular to the applied field direction. The magnetization versus temperature data with a measuring field of 0.05 T obtained under the Zero Field Cooled (ZFC) and field cooled (FC) protocols are shown in Fig.2. It is seen from the figure that there is clear bifurcation of the ZFC and FC curves indicative of a phase transition at 15 K. This magnetization anomaly, however, becomes a broad cusp, under large measuring magnetic field of 4T, implying that the transition is antiferromagnetic in nature, similar to that observed in Fe compound [11]. In addition, the low temperature step like increase at ~ 8 K in magnetization seen the FC data at upto 0.1 T, gets smeared to a monotonic increase with decrease in temperature. The results of isothermal magnetization as a function of magnetic field are displayed in various panels in Fig.3. In the low field region, a jump in magnetization is seen, whereas, at higher fields the M versus H is linear, characteristic of the antiferromagnetic nature of the magnetic ground state [11]. As seen in the measurements in the Fe compound [11], the low field jump in magnetization can arise due to free spins aligning easily with an applied magnetic field. Thus from our measurements, it can be inferred that the presence of two coexisting magnetic phases, could be a generic feature in all the transition metal compounds belonging to the class $[(CH_3)_2NH_2]M(HCOO)_3$ where M is a magnetic transition metal ion.

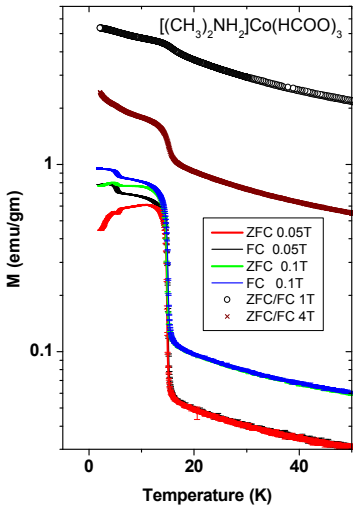

Fig.2 The magnetization versus temperature in the 1.6 to 50 K temperature range, with measuring fields indicated, ZFC and FC curves are separated for measuring fields of 0.1 T and 0.05 T.

To get an insight into the transitions observed in magnetization measurements, we performed specific heat measurements on the small, single-crystal, of $[(CH_3)_2NH_2]Co(HCOO)_3$ as a function of temperature, in various magnetic fields. The as-measured specific heat data, displayed in Fig.4, shows a sharp lambda like transition at 15 K, corresponding with the magnetic transition (cf. Fig. 2), similar to that reported for the Mn system [7]. It is evident from the figure that the specific heat peak that occurs at 15 K, shifts to lower temperature and the area under the specific heat curve reduces with

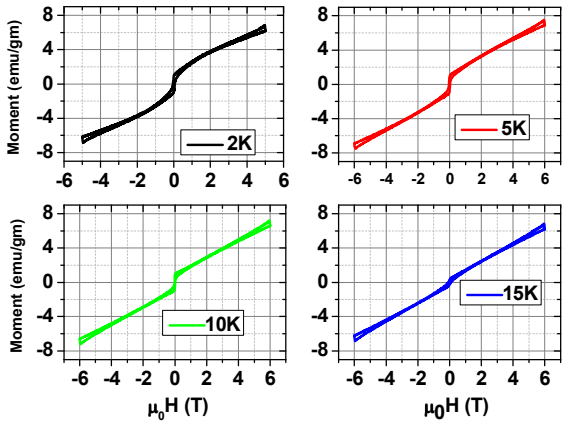

Fig.3 Isothermal Magnetisation versus magnetic field measured at the temperatures indicated. The M versus H shows a jump at low field superimposed on a linear variation, the former associated with the single-ion magnet and the latter with long range anti-ferromagnetism.

the application of magnetic field. To extract the enthalpy change from the specific heat data, across the magnetic transition, a polynomial background function is first subtracted from the specific heat versus temperature plot and peak area evaluated. The variation of enthalpy change obtained at the magnetic phase transition, is plotted as a function of applied magnetic field in Fig.5. Given the two phase magnetic structure of the sample below 15 K, as inferred from the isothermal magnetization studies indicated above, the observed decrease in the enthalpy change with the applied field reflects the decrease in the volume fraction of the antiferromgnetic phase and the corresponding build up of single-ion magnetic structure. It must be mentioned that a similar specific heat anomaly at the magnetic transition, was earlier observed [7] in a mosaic of single crystals of $[(CH_3)_2NH_2]Mn(HCOO)_3$, which was attributed to the suppression of the antiferromagnetic transition with the applied magnetic field. We note from Fig. 4.,that while there is a marginal decrease in the antiferromagnetic transition temperature with the applied field, there is a significant change in the enthalpy across the transition which suggests that the explanation in terms of the changing volume fraction of two phase magnetic structure is more tenable.

The results of specific heat measurements, across the order- disorder transition at ~ 160 K, is shown in Fig. 6a., after background subtraction. It is seen that there is considerable hysteresis in the heating and cooling runs, pointing to the first order nature of the transition. Fig.6a also indicates that the transition is insensitive to the applied field. Similar specific heat anomalies has been seen earlier in Mn[7] Zn and Fe formamide [20] and has been attributed structural transition, associated with the orientational ordering of N. The most definitive evidence for the ordering of N atoms leading to the structural transition has been obtained from temperature dependent Raman spectroscopy experiments in the Fe and Zn

formamides [22]. Following this, we have carried out Raman measurements as a function of temperature in the Co-formamide system, and the results at two representative temperatures of 200 and 100 K are shown in Fig. 6b. It is seen that the characteristic mode corresponding to HCOO is seen to split at low temperatures, consistent with that observed in the Zn formamide [22], implying the specific heat anomaly indeed arises due to a structural transition in the $[(CH_3)_2NH_2]Co(HCOO)_3$ crystals.

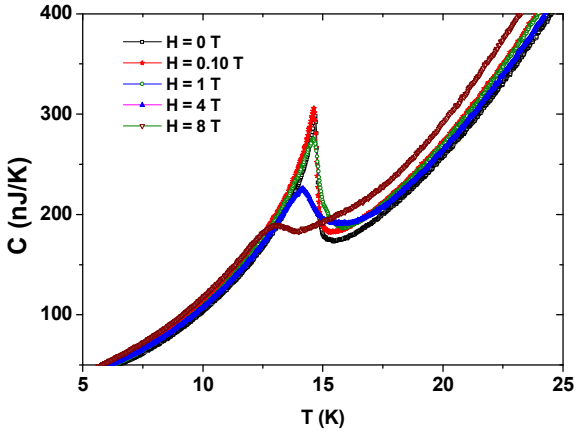

Fig.4. Heat capacity measurements on a single crystal of $[(CH_3)_2NH_2]Co(HCOO)_3$ at various applied magnetic fields as indicated. The peak in heat capacity corresponds to the magnetic transition seen in Fig. 2. A suppression of the peak temperature and broadening of the transition is evident with increase in the strength of the external magnetic field.

In Fig.7, we plot the ZFC magnetisation data measured in the SQUID-VSM in the high temperature range, across the structural transition, for measuring fields of 1 T and 4 T. It is seen that there is a distinct jump in the magnetization at 157 K, the temperature that corresponds to the structural transition, riding on the Curie-Weiss behavior. This jump in magnetization is seen for the first time in this family of formamides, and not reported for the Mn, Fe and Ni systems [20], and may be linked to a possible change in the magnetic moment of the Co^{2+} ion. In order to explore this, we estimate the Curie constant from DC magnetisation measurements, at measuring fields of 0.1T and 0.5T, carried out on an assemblage of embedded in GE vanish. The results of magnetisation versus inverse temperature below and above the transition, is shown in Fig.8. The magnetic moments obtained from the Curie- Weiss fits are estimated to be 4.07 μB below and 4.63 μB above the transition. We note that these values of the magnetic moments fall in the range corresponding to a high spin state of Co^{2+} ion[23], and thus the marginal increase with temperature could be due to changes in the distribution of the ligands around Co^{2+} ions across the transition.

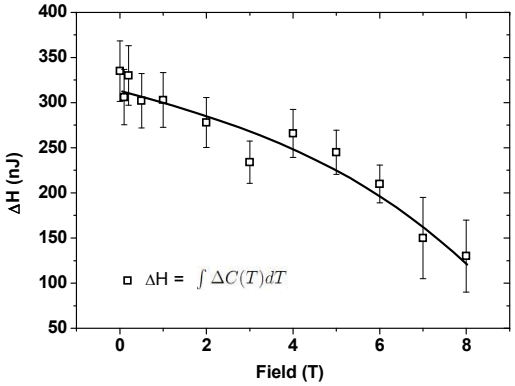

Fig.5. Decrease in the enthalpy change across the antiferromagnetic magnetic transition, with the applied magnetic field. The enthalpy change is obtained by integrating the area under the heat capacity curve, shown in Fig.4, after a polynomial fitted background subtraction.

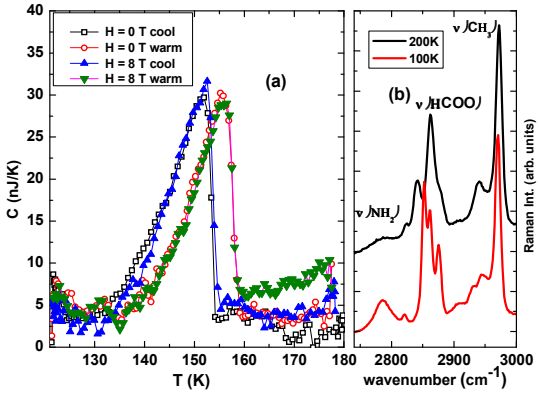

Fig.6.(a). Variation in heat capacity across the order-disorder transition in $[(CH_3)_2NH_2]Co(HCOO)_3$ crystal. The large hysteresis between the heating and cooling cycles is clearly seen. The applied magnetic field (8 T) has no effect on the transition temperature.(b)Raman spectra in the crystal in the 2750 to 3000 cm^{-1} range at 100 and 200K,. The splitting of the HCOO mode and the development of the NH_3 mode at low temperature is clearly seen.

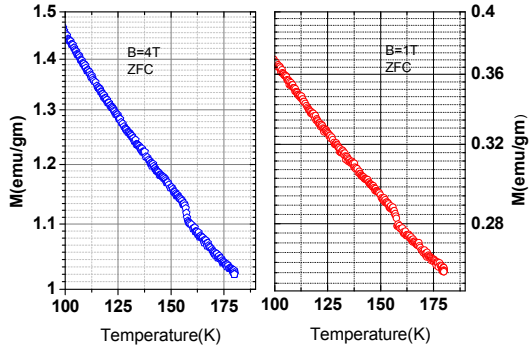

Fig.7 Magnetization versus temperature measured on a single crystal at 4T and 1T in the ZFC protocol showinga jump in magnetisationcoinciding with the structural transition.

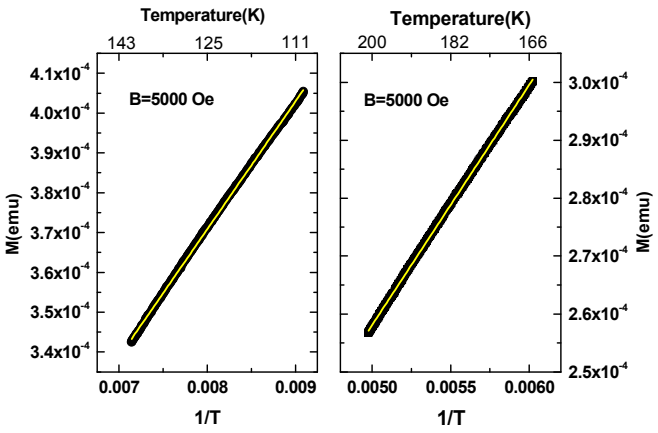

Fig.8. Curie Weiss fit (yellow) to DC magnetisation versus inverse temperature data (black band) below and above the structural transition, obtained at a measuring field of 5000 Oe from SQUID-VSM measurements.

Conclusions

Temperature dependent magnetization and hysteresis measurements in the MOF crystal $[(CH_3)_2NH_2]Co(HCOO)_3$, suggest the existence of a two phase magnetic structure within the canted antiferromagnetic phase – as has been reported in Fe system [11]. Evidence for the presence of two co-existing phases is bolstered by the results of specific heat measurements across the magnetic transition at 20 K, in the presence of external magnetic field. In the paramagnetic phase across the structural transition at ~ 160 K, a jump in the magnetization has been seen can be attributed to magnetic moment change of Co^{2+}.

Acknowledgements

The authors gratefully acknowledge Dr. A.K Sinha for XRD measurements at the BL-12 beamline of the Indus-II synchrotron. The authors thank Dr. G. Amarendra for making available the SQUID-VSM at the UGC-DAE-CSR node at Kalpakkam for the magnetization measurements.

Notes and references

[a]Materials Science Group, IGCAR, Kalpakkam, INDIA 603102
[b]Department of Chemistry, Indian Institute of Technology, Kanpur, INDIA 208016

.

1 O. M. Yaghi, G. M. Li, and H. L. Li, *Nature* (London) 1995, **378**, 703
2 *Functional Metal-Organic Frameworks: Gas Storage,Separation and Catalysis*, Ed. Martin Schroder, Topics in Current Chemistry, vol 293 Springer Verlag (2010)
3 *Metal-Organic Frameworks: Design and application*, Edited by Leonard R. MacGillivray, John Wiley and sons (2010)
4 R. J. Kuppler, D. J. Timmons, Q. R. Fang, J. R. Li, T. A. Makala, M. D. Young, D. Yuan, D. Zhao, W. Zhuang, H. C. Zhou, *Coordination, Chem. Rev.*, 2009, **253**, 3042.
5 C.N.R. Rao, A. K. Cheetham and A. Thirumurugan, J. *Phys.: Condens. Matter,* 2008, **20**, 083202
6 X.Y. Wang, L. Gan, S.W. Zhang, and S.Gao, *Inorg. Chem.*, 2004, **43**, 4615
7 P. Jain, V. Ramachandran, R.J. Clark, H.D. Zhou, B.H. Toby, N.S. Dalal, H.W. Kroto, A.K. Cheetham, J. Am. Chem. Soc. 2009, **131**13625.
8 W. Wang L. Q. Yan, J. Z. Cong, Y. L. Zhao, F. Wang, S. P. Shen, T. Zou, D. Zhang, S. G. Wang, X. -F. Han & Y. Sun,*Scientific Reports,* 2013, | 3 : 2024 | DOI: 10.1038/srep02024
9 W.Li, Z. Zhang, E. G. Bithell, A. S. Batsanov , P. T. Barton, P.J. Saines, P. Jain, C. J. Howard , M. A. Carpenter, A. K. Cheetham, *ActaMaterialia*2013, **61**, 4928.
10 Z. Wang, P. Jain, K.YongChoi,Johan van Tol,A.K. Cheetham, H.W. Kroto, H.J. Koo, H. Zhou, J. Hwang, Eun Sang Choi,Myung-Hwan Whangbo ,and N. S. Dalal, *Physical Review* B. 2013, **87**, 224406.
11 Ying Tian, Wei Wang, Yisheng Chai, Junzhuang Cong, ShipengShen, LiqinYan,Shouguo Wang, Xiufeng Han, and Young Sun, Phys. Rev. Lett. 112, 017202 (2014)
12 Y. Tian, J. Cong, S. Shen, Y. Chai, L. Yan, S. Wang, and Young Sun,*Phys. Status Solidi RRL*, 2013, 1–4 / **DOI** 10.1002/pssr.201308230
13 Ying Tian, Alessandro Stroppa, Yisheng Chai, Liqin Yan, Shouguo Wang, Paolo Barone, Silvia Picozzi and Young Sun, *Scientific Reports,* 2 | 4 : 6062 | DOI: 10.1038/srep06062(August14) 2014
14 M. W. Haverkort, Z. Hu, J. C. Cezar, T. Burnus, H. Hartmann, M. Reuther, C. Zobel, T. Lorenz, A. Tanaka, N. B. Brookes, H. H. Hsieh, H.-J. Lin, C. T. Chen, and L. H. Tjeng, *Phys. Rev. Lett.* **97**, 176405 (2006)
15 Keiichiro Nakamura, RuiGoto, Kunihide Okada, MuneakiFujii, Physica B **329–333,** 719–720 (2003)
16 A. K. Sinha, A. Sagdeo, P. Gupta, A. Kumar, M. N. Singh, R. K. Gupta, S.K. Kane and S. K. Deb *AIP Conference Proceedings***1349** 503-4 (2011)
17 A. P.Hammersley, S. O.Svensson, M.Hanfland, A. N.Fitch and D.Hausermann *High Pressure Research***14** 235-48 (1996).
18 Toby B *Journal of Applied Crystallography,* 2001, **34**, 210.
19 A C Larson and R B Von Dreele *Los Alamos National Laboratory Report LAUR*1994, **86**, 748.
20 P. Jain, *Multiferroic Metal Organic Frameworks with Perovskite Architecture,* Ph.D thesis (Florida State University,2010).
21 A.A.Minokov, S. B. Roy, Y.V. Bugoslavsky and L. F. Cohen, *Review of Scientific instruments*, 2005, **76**, 043906.
22 M. Maczka, M. Ptak, L. Macalik, Vibrational Spectroscopy **71,** 98 (2014)
23 J.H.Huheey, E.A.Keiter and R.L.Keiter, Inorganic Chemistry, Principles of Structure and reactivity, p 465, Pearson Education, Inc. (2000)